4. Merrilees MA, Scott PJ, Romo M. Five-year survival of 728 patients after myocardial infarction: A community study. *Br Heart J* 1980; **43:** 176–183.
5. Vakili BA, Kaplan RC, Brown DL. Sex-based differences in early mortality of patients undergoing primary angioplasty for first acute myocardial infarction. *Circulation* 2001; **104:** 3034–3038.
6. Kudenchuk PJ, Maynard C, Martin JS, Wirkus M, Weaver WD. Comparison of presentation, treatment, and outcome of acute myocardial infarction in men versus women (the Myocardial Infarction Triage and Intervention Registry). *Am J Cardiol* 1996; **78:** 9–14.
7. Chandra NC, Ziegelstein RC, Rogers WJ, Tiefenbrunn AJ, Gore JM, French WJ, et al. Observations of the treatment of women in the United States with myocardial infarction: A report from the National Registry of Myocardial Infarction-I. *Arch Intern Med* 1998; **158:** 981–988.
8. Marso SP, Gowda M, O'Keefe JH, Coen MM, McCallister BD, Giorgi LV, et al. Improving in-hospital mortality in the setting of an increasing risk profile among patients undergoing catheter-based reperfusion for an acute myocardial infarction without cardiogenic shock. *J Invasive Cardiol* 2003; **15:** 711–716.
9. Dittrich H, Gilpin E, Nicod P, Cali G, Henning H, Ross J Jr. Acute myocardial infarction in women: Influence of gender on mortality and prognostic variables. *Am J Cardiol* 1988; **62:** 1–7.
10. Tamis-Holland JE, Palazzo A, Stebbins AL, Slater JN, Boland J, Ellis SG, et al. Benefits of direct angioplasty for women and men with acute myocardial infarction: Results of the Global Use of Strategies to Open Occluded Arteries in Acute Coronary Syndromes Angioplasty (GUSTO II-B) Angioplasty Substudy. *Am Heart J* 2004; **147:** 133–139.
11. Lansky AJ, Pietras C, Costa RA, Tsuchiya Y, Brodie BR, Cox DA, et al. Gender differences in outcomes after primary angioplasty versus primary stenting with and without abciximab for acute myocardial infarction: Results of the Controlled Abciximab and Device Investigation to Lower Late Angioplasty Complications (CADILLAC) trial. *Circulation* 2005; **111:** 1611–1618.
12. Oe K, Shimizu M, Ino H, Yamaguchi M, Terai H, Hayashi K, et al. Effects of gender on the number of diseased vessels and clinical outcome in Japanese patients with acute coronary syndrome. *Circ J* 2002; **66:** 435–440.
13. Yarzebski J, Col N, Pagley P, Savageau J, Gore J, Goldberg R. Gender differences and factors associated with the receipt of thrombolytic therapy in patients with acute myocardial infarction: A community-wide perspective. *Am Heart J* 1996; **131:** 43–50.
14. Kostis JB, Wilson AC, O'Dowd K, Gregory P, Chelton S, Cosgrove NM, et al. Sex differences in the management and long-term outcome of acute myocardial infarction: A statewide study. MIDAS Study Group: Myocardial Infarction Data Acquisition System. *Circulation* 1994; **90:** 1715–1730.
15. Kosuge M, Kimura K, Kojima S, Sakamoto T, Ishihara M, Asada Y, et al. Beneficial effect of preinfarction angina on in-hospital outcome is preserved in elderly patients undergoing coronary intervention for anterior acute myocardial infarction. *Circ J* 2005; **69:** 630–635.
16. The TIMI study group. The Thrombolysis in Myocardial Infarction (TIMI) trial. *N Engl J Med* 1985; **312:** 932–936.
17. Mehilli J, Ndrepepa G, Kastrati A, Nekolla SG, Markwardt C, Bollwein H, et al. Gender and myocardial salvage after reperfusion treatment in acute myocardial infarction. *J Am Coll Cardiol* 2005; **45:** 828–831.
18. Weaver WD, Simes RJ, Betriu A, Grines CL, Zijlstra F, Garcia E, et al. Comparison of primary coronary angioplasty and intravenous thrombolytic therapy for acute myocardial infarction: A quantitative review. *JAMA* 1997; **278:** 2093–2098.
19. Capes SE, Hunt D, Malmberg K, Gerstein HC. Stress hyperglycemia and increased risk after myocardial infarction in patients without diabetes: A systematic overview. *Lancet* 2000; **355:** 773–778.
20. Wahab NN, Cowden EA, Pearce NJ, Gardner MJ, Merry H, Cox JL; ICONS Investigators. Is blood glucose an independent predictor of mortality in acute myocardial infarction in the thrombolytic era? *J Am Coll Cardiol* 2002; **40:** 1748–1754.
21. Sadeghi HM, Stone GW, Grines CL, Mehran R, Dixon SR, Lansky AJ, et al. Impact of renal insufficiency in patients undergoing primary angioplasty for acute myocardial infarction. *Circulation* 2003; **108:** 2769–2775.
22. Kosuge M, Kimura K, Kojima S, Sakamoto T, Matsui K, Ishihara M, et al. Effects of glucose abnormalities on in-hospital outcome after coronary intervention for acute myocardial infarction. *Circ J* 2005; **69:** 375–379.

ELSEVIER

International Journal of Cardiology 106 (2006) 177–182

International Journal of Cardiology

www.elsevier.com/locate/ijcard

Determinants of rapid progression of aortic root dilatation and complications in Marfan syndrome[B]

Aleksandar M. Lazarevic[a], Satoshi Nakatani[a,T], Yutaka Okita[b], Jelena Marinkovic[c], Yutaka Takeda[a], Keiji Hirooka[a], Hiroshi Matsuo[a], Soichiro Kitamura[b], Masakazu Yamagishi[a], Kunio Miyatake[a]

[a]*Department of Cardiology, National Cardiovascular Center, Suita, Osaka, Japan*
[b]*Department of Cardiothoracic Surgery, National Cardiovascular Center, Suita, Osaka, Japan*
[c]*Cardiovascular Research Center, Dedinje Cardiovascular Institute, Belgrade University Medical School, Belgrade, Serbia and Montenegro*

Received 3 August 2004; received in revised form 20 January 2005; accepted 28 January 2005
Available online 30 March 2005

ELSEVIER

International Journal of Cardiology 106 (2006) 177–182

International Journal of Cardiology

www.elsevier.com/locate/ijcard

Determinants of rapid progression of aortic root dilatation and complications in Marfan syndrome☆

Aleksandar M. Lazarevic[a], Satoshi Nakatani[a,*], Yutaka Okita[b], Jelena Marinkovic[c], Yutaka Takeda[a], Keiji Hirooka[a], Hiroshi Matsuo[a], Soichiro Kitamura[b], Masakazu Yamagishi[a], Kunio Miyatake[a]

[a]*Department of Cardiology, National Cardiovascular Center, Suita, Osaka, Japan*
[b]*Department of Cardiothoracic Surgery, National Cardiovascular Center, Suita, Osaka, Japan*
[c]*Cardiovascular Research Center, Dedinje Cardiovascular Institute, Belgrade University Medical School, Belgrade, Serbia and Montenegro*

Received 3 August 2004; received in revised form 20 January 2005; accepted 28 January 2005
Available online 30 March 2005

Abstract

Background: Progressive aortic dilatation has prognostic significance in the Marfan syndrome.
Methods: To identify which patients were at high risk of rapid progression, we echocardiographically studied 43 patients (age 22 ± 14 years) with the mean follow-up period of 5.2 ± 3.2 years. Aortic diameters, left ventricular (LV) size, fractional shortening, and the severity of aortic and mitral regurgitation were assessed. Transmitral peak early and atrial flow velocities, their ratio and the deceleration time of peak early velocity were also obtained.
Results: Mean annual increases of aortic diameters were 0.4 ± 0.3 mm at the annulus, 1.5 ± 1.3 mm at the sinuses of Valsalva, 0.7 ± 0.6 mm at the supraaortic ridge and 0.4 ± 0.4 mm at the proximal ascending aorta. Patients were divided into 2 groups according to the aortic growth rate at the sinuses of Valsalva level: rapid (R, >3% per year, 15 patients) or slow (S, ≤3% per year, 28 patients) progression groups. Measured variables did not show significant differences between the 2 groups except older age, higher blood pressure and more severe aortic regurgitation in group R. Multiple regression analysis identified prolonged deceleration time as the most important variable predicting aortic complications. Aortic dissection occurred more frequently in group R (7 patients, 47%) than in group S (0%, P<0.001).
Conclusions: Marfan patients at older age, with higher blood pressure, and with significant aortic regurgitation were at high risk of progression of aortic dilatation, with the most remarkable increase at the sinuses of Valsalva. Prolonged deceleration time may relate to an increased risk for aortic complications.
© 2005 Elsevier Ireland Ltd. All rights reserved.

Keywords: Marfan syndrome; Echocardiography; Aortic dissection; LV function

1. Introduction

One of the most serious clinical manifestations of the Marfan syndrome is progressive aortic root dilatation which may lead to aortic dissection, rupture or regurgitation that are responsible for decreased life expectancy in these patients [1–4]. Although aortic root dilatation is observed in 60–80% of Marfan patients [5–7], aortic growth rate among individuals may vary [8] and factors predicting the rate of change of the aortic diameter are still not completely

☆ Dr. Lazarevic was supported by a scholarship from the Ministry of Education, Science and Culture of Japan, Tokyo, Japan. This study was partly supported by a Research Grant from the Ministry of Health, Labor and Welfare, Japan.
* Corresponding author. Department of Cardiology National Cardiovascular Center 5-7-1 Fujishiro-dai, Suita Osaka 565-8565, Japan. Tel.: +81 6 6833 5012; fax: +81 6 6872 7486.
E-mail address: nakatas@hsp.ncvc.go.jp (S. Nakatani).

0167-5273/$ - see front matter © 2005 Elsevier Ireland Ltd. All rights reserved.
doi:10.1016/j.ijcard.2005.01.040

clarified. It would be clinically important to define which patients are at high risk of rapid progression.

Several factors have been reported to relate to aortic complications in the Marfan syndrome including aortic size, systolic blood pressure and aortic growth rate [8]. However, determinants of aortic growth rate remains elusive. Because the abnormality in extracellular connective tissue matrix in the Marfan syndrome [9] involves not only aorta but also heart muscle [10], left ventricular (LV) systolic and diastolic function may have some influence on aortic growth rate and complications. In the present study, we investigated determinants of rapid progression of aortic root dilatation and aortic complications with a special interest of the effect of LV function on them. Further, we clarified characteristics of patients who might have poor prognosis.

2. Materials and methods

2.1. Study population

We studied retrospectively 114 consecutive patients with the Marfan syndrome or relatives of patients, who underwent clinical and echocardiographic examinations. Inclusion criteria were: (1) positive strict, internationally established diagnostic criteria [11,12] for the Marfan syndrome, (2) echocardiographic follow-up ≥ 1 year (2-dimensional echocardiography and Doppler color flow mapping), and (3) no proximal aortic surgery before the initial examination. The final study group included 43 patients (age 22 ± 14 years [range 1–59 years], 23 males), with the mean follow-up period of 5.2 ± 3.2 years (range 1–10 years).

2.2. Echocardiography

Two-dimensional, M-mode and Doppler echocardiograms were obtained with a commercially available cardiac ultrasound system, using a 2.5-MHz transducer and stored on videotape and/or strip chart for later analysis. Aortic root measurements were made in 2-dimensional parasternal long-axis view at end-diastole at 4 levels: aortic annulus, sinuses of Valsalva, supraaortic ridge and proximal ascending aorta 1–2 cm above the supraaortic ridge according to the method of Roman et al. (Fig. 1) [13]. All measurements were made using the leading edge technique on up to 5 cycles and averaged. The echocardiographic evidence of aortic root dilatation was determined using Roman's nomograms based on age and body surface area [13]. Dimensions of the sinuses of Valsalva and supraaortic ridge were used to determine an aortic ratio as follows:

$$\text{Aortic ratio} = \frac{\text{measured diameter}}{\text{expected diameter}}$$

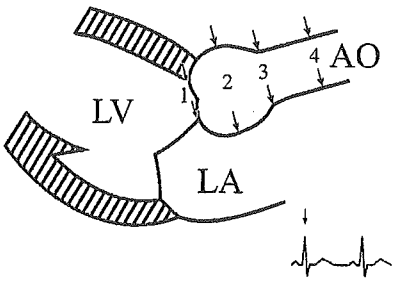

Fig. 1. Schematic illustration of the long-axis two-dimensional echocardiogram. Aortic root measurements were obtained at 4 levels, including; 1) the annulus, 2) sinuses of Valsalva, 3) supraaortic ridge and 4) proximal ascending aorta. AO=aorta; LA=left atrium; LV=left ventricle.

where the expected diameter was obtained using the regression equation derived from Roman's nomograms [13]. The mean annual rate of aortic root dilatation was determined by dividing the absolute change in aortic diameter between the final and initial echocardiograms by the duration of follow-up in years. We also assessed the annual change in the aortic ratio by dividing the change in aortic ratio between the final and initial echocardiograms by the time interval between them. The severity of aortic regurgitation and mitral regurgitation was graded semi-quantitatively (1–4) using color Doppler jet area criteria [14–16]. Echocardiographic evidence of mitral valve prolapse was evaluated using established echocardiographic criteria [17]. LV end-diastolic and end-systolic diameters, fractional shortening, and diastolic interventricular septum and LV posterior wall thicknesses were determined according to the recommendations of the American Society of Echocardiography [18]. Standard pulsed wave Doppler flow velocities measurements were obtained from the apical long-axis view, with the sample volume placed at the level of the mitral valve leaflet tips. The following Doppler indexes were measured: peak early (E) and atrial (A) transmitral filling velocities, E deceleration time and E/A ratio. A single investigator (A.M.L) blinded to the clinical data performed the off-line analysis.

2.3. Statistical analysis

Results are reported as mean value $\pm$ SD. Comparison of data between patients groups was performed by use of a two-tailed, unpaired Student's t test or Mann–Whitney U test. Mean annual increases at the aortic root levels were compared using analysis of variance. The χ^2 test (with continuity correction when applicable) was used to compare frequencies among the patients groups. Multivariate and univariate linear regression analysis was used to evaluate which variables such as blood pressure, heart rate, LV diameter indexes, fractional shortening, aortic regurgitation and LV diastolic filling indexes correlated best with the progression of aortic root dilatation. Independence of relation was tested using logistic regression. Significance was established at $P<0.05$.

3. Results

3.1. Changes in aortic diameters and grouping of patients

Because of suboptimal images, measurements at the supraaortic ridge level and those at the ascending aorta level were not available in 5 and 11 patients, respectively. Aortic diameters increased with time (Fig. 2). Mean annual increases were 0.4 ± 0.3 mm at the level of annulus, 1.5 ± 1.3 mm at the level of the sinuses of Valsalva, 0.7 ± 0.6 mm at the supraaortic ridge and 0.4 ± 0.4 mm at the proximal ascending aorta. The most rapid change was seen at the sinuses of Valsalva diameter ($F=17$, $P<0.001$ vs. 3 other aortic diameters). The change in aortic ratio was also the highest at the level of the sinuses of Valsalva ($3 \pm 4\%$ per year). Because the annual changes in aortic root diameters were most prominent at the aortic sinus level, patients were divided into 2 groups according to the mean annual change in aortic ratio at the sinuses of Valsalva: rapid (R, >3% per year, 15 patients) or slow (S, ≤3% per year, 28 patients) progression groups. During the follow-up period, 7 patients in group R had aortic dissection requiring aortic surgery and 2 patients died. One patient died 2 months after aortic root and valve replacement and another patient died 3 years after Bentall's operation from colon cancer. Aortic dissection [2 proximal (involving the ascending aorta) and 5 distal (all dissections that originate after the left subclavian artery)] occurred more frequently in group R (7 patients, 47%) than in group S (0%, $\chi^2=12.37$, $P<0.001$). Only 1 patient from group S underwent prophylactic aortic root and valve replacement due to ascending aortic aneurysm and severe aortic regurgitation.

3.2. Characteristics of the patients

Demographic and clinical data for all 43 patients at the time of the initial examination are described in Table 1. Patients in group R were older than those in group S ($P<0.01$). There were no significant differences in sex, heart rate and body surface area, but systolic ($P<0.02$) and diastolic ($P<0.05$) blood pressures were higher in group R.

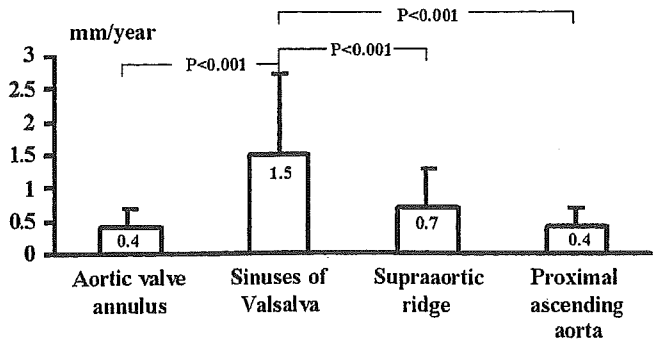

Fig. 2. Mean annual increases of aortic root diameter at 4 levels in all study patients.

Table 1
Demographic and clinical data in all study patients and in the slow (S) and rapid (R) progression group at entry

	Total ($n=43$)	Group S ($n=28$)	Group R ($n=15$)
Age (years)	22 ± 14	18 ± 12	30 ± 15*
Male sex	23 (53%)	14 (50%)	9 (60%)
Body surface area (m^2)	1.56 ± 0.37	1.51 ± 0.4	1.67 ± 0.2
Heart rate (beats/min)	73 ± 8	72 ± 7	75 ± 9
Blood pressure (mm Hg)			
Systolic	117 ± 15	112 ± 13	124 ± 16†
Diastolic	67 ± 9	65 ± 8	70 ± 9‡
Pulse pressure	50 ± 12	48 ± 11	54 ± 13
Mitral valve prolapse	24 (56%)	17 (61%)	7 (47%)
Aortic root dilatation	40 (93%)	26 (93%)	14 (93%)
Duration of follow-up (years)	5.2 ± 3.2	6.3 ± 3.1	3.3 ± 2.5§

*$P<0.01$; †$P<0.02$; ‡$P<0.05$; §$P<0.005$ compared with group S. Data presented are mean value ± SD or number (%) of patients.

Pulse pressure was comparable between the 2 groups. Aortic root dilatation was similarly seen in group R and in group S. The presence of mitral valve prolapse was comparable in both groups. Duration of follow-up was shorter in group R ($P<0.005$). There were no differences in the incidence of patients using β-adrenergic blocking drugs between the 2 groups.

3.3. Echocardiographic data (Table 2)

At the initial examination mean aortic sinus diameter ($P=0.001$) and aortic ratio ($P=0.01$) were larger in group R. LV diameters and fractional shortening were comparable between the 2 groups, but LV wall thickness was larger in group R ($P=0.01$ for interventricular septum and $P=0.02$ for posterior wall). Aortic regurgitation was more common ($P=0.001$) and more severe in group R ($P=0.02$). The prevalence ($P=0.349$) and severity of mitral regurgitation ($P=0.13$) was comparable in both groups (Table 2).

Echocardiographic data at the most recent follow-up or before surgery showed no significant differences in LV diameters, fractional shortening and severity of mitral regurgitation between groups R and S. However, aortic sinus diameter ($P<0.001$) and aortic ratio ($P<0.001$) were larger and aortic regurgitation was more severe in group R ($P<0.001$).

Pulsed Doppler indexes were obtained in 27 out of 43 patients (12 patients in group R and in 15 patients in group S) (Table 3). At the time of the initial pulsed Doppler examination, there were no differences in age (30 ± 14 vs. 27 ± 12 years), blood pressures (125 ± 28 vs. 117 ± 11 mm Hg for systolic pressure and 69 ± 9 vs. 68 ± 8 mm Hg for diastolic pressure), LV dimensions (29 ± 4 vs. 30 ± 4 mm/m^2 for end-diastolic diameter index and 18 ± 4 vs. 19 ± 3 mm/m^2 for end-systolic diameter index), fractional shortening ($37 \pm 5\%$ vs. $36 \pm 3\%$), LV wall thickness (8.4 ± 1.4 vs. 9.2 ± 1.6 mm for interventricular septum and 8.1 ± 1.2 vs. 8.8 ± 1.5 for posterior wall) and the severity of aortic

Table 2
Echocardiographic variables

	Total ($n=43$)		Group S ($n=28$)		Group R ($n=15$)	
	Initial	Follow-up	Initial	Follow-up	Initial	Follow-up
Aortic sinus diameter (mm)	36.8 ± 8.7	43.2 ± 11.5	33.7 ± 7.2	39 ± 7	42.7 ± 8.4*	51 ± 14†
Aortic sinus ratio	1.36 ± 0.23	1.49 ± 0.32	1.30 ± 0.20	1.37 ± 0.2	1.48 ± 0.24‡	1.72 ± 0.4†
LV EDD (mm)	48 ± 7	52 ± 8	47 ± 8	51 ± 8	50 ± 5	54 ± 9
LV EDDI (mm/m^2)	32 ± 8	32 ± 6	33 ± 9	31 ± 6	31 ± 6	33 ± 7
LV ESD (mm)	31 ± 5	34 ± 7	30 ± 6	33 ± 6	32 ± 4	35 ± 8
LV ESDI (mm/m^2)	21 ± 5	21 ± 5	21 ± 6	20 ± 4	20 ± 5	22 ± 6
FS (%)	36 ± 4	34 ± 5	36 ± 4	34 ± 5	36 ± 5	34 ± 5
IVS (mm)	8.1 ± 1.8	8.6 ± 1.6	7.6 ± 1.6	8.3 ± 1.5	9.0 ± 1.7‡	9.2 ± 1.7
PW (mm)	7.7 ± 1.7	8.3 ± 1.5	7.3 ± 1.5	7.9 ± 1.4	8.5 ± 1.8§	8.9 ± 1.6‖
Aortic regurgitation						
Prevalence	16 (37%)	22 (51%)	5 (18%)	8 (29%)	11 (73%)*	14 (93%)†
Severity	0.5 ± 0.8	0.9 ± 1.2	0.3 ± 0.8	0.4 ± 0.9	0.9 ± 0.7§	1.9 ± 1.1†
Mitral regurgitation						
Prevalence	12 (28%)	19 (44%)	6 (21%)	11 (39%)	6 (40%)	8 (53%)
Severity	0.4 ± 0.7	0.8 ± 1.1	0.2 ± 0.5	0.6 ± 1.0	0.7 ± 1.0	1.0 ± 1.2

*$P=0.001$; †$P<0.001$; ‡$P=0.01$; §$P=0.02$; ‖$P=0.04$ compared with group S. Data presented are mean value ± SD or number (%) of patients. EDD=end-diastolic diameter; EDDI=end-diastolic diameter index, ESD=end-systolic diameter; FS=fractional shortening; IVS=diastolic interventricular septum thickness; PW=diastolic LV posterior wall thickness.

regurgitation (0.7 ± 0.5 vs. 0.5 ± 1.0) and mitral regurgitation (0.7 ± 1.0 vs. 0.2 ± 0.5) between the 2 groups. However, patients in group R showed longer deceleration time ($P=0.005$), lower E ($P=0.015$) and lower E/A ($P=0.002$) compared to those in group S. A wave velocity did not differ significantly between the 2 groups. Follow-up data were available in 17 patients. At the most recent follow-up, deceleration time was longer in group R ($P=0.03$). Other Doppler indexes were comparable between the 2 groups.

3.4. Possible predictors of rapid progression of aortic root dilatation

To identify possible predictors of rapid aortic root dilatation, we performed multiple regression analyses. Aortic root dilatation at the sinuses of Valsalva level and that at the supraaortic ridge level were determined by diastolic pressure (t value=2.091, $P=0.043$ for the sinus level, t value=2.348, $P=0.024$ for the supraaortic ridge level). Changes of aortic ratios at the sinus and supraaortic ridge levels were influenced by diastolic pressure and aortic regurgitation (t value=2.340, $P=0.024$ and t value=2.163, $P=0.037$ for the aortic sinus, and t value=3.374, $P=0.002$ and t value=3.438, $P=0.002$ for the supraaortic ridge). Fig. 3 shows t values of each parameter to predict aortic growth rate with overall multiple correlation coefficient.

Multivariate logistic regression analysis was used to identify the best predictor of rapid aortic dilatation (group R patients). In this analysis, the parameters which differed significantly between groups R and S at initial evaluation were included. They were aortic sinus diameter, aortic sinus ratio, systolic and diastolic blood pressures, degree of aortic regurgitation, deceleration time, E and E/A. The only independent predictor of rapid dilatation was E/A ratio ($P=0.0223$). We also assessed the independent predictors of aortic complications using the logistic regression with the same parameters. The only independent predictor of aortic complications was deceleration time ($P=0.0295$).

4. Discussion

4.1. Features of the patients with rapid progression of the aortic root dilatation

The present study showed that the Marfan patients at older age, with higher blood pressure, and with significant aortic regurgitation were at high risk of rapid progression of

Table 3
Doppler left ventricular diastolic filling variables

	Total		Group S		Group R	
	Initial ($n=27$)	Follow-up ($n=17$)	Initial ($n=15$)	Follow-up ($n=8$)	Initial ($n=12$)	Follow-up ($n=9$)
DT	184 ± 26	196 ± 40	172 ± 15	175 ± 22	199 ± 30*	216 ± 43†
E	62 ± 15	57 ± 14	68 ± 13	63 ± 13	54 ± 14‡	51 ± 14
A	44 ± 13	44 ± 9	40 ± 14	42 ± 10	48 ± 12	46 ± 8
E/A	1.55 ± 0.58	1.35 ± 0.45	1.84 ± 0.57	1.55 ± 0.36	1.19 ± 0.35§	1.18 ± 0.46

*$P=0.005$; †$P=0.03$; ‡$P=0.015$; §$P=0.002$ compared with group S. Data presented are mean value ± SD or number of patients. A=atrial diastolic filling velocity; DT=deceleration time of the early diastolic filling velocity; E=early diastolic filling velocity.

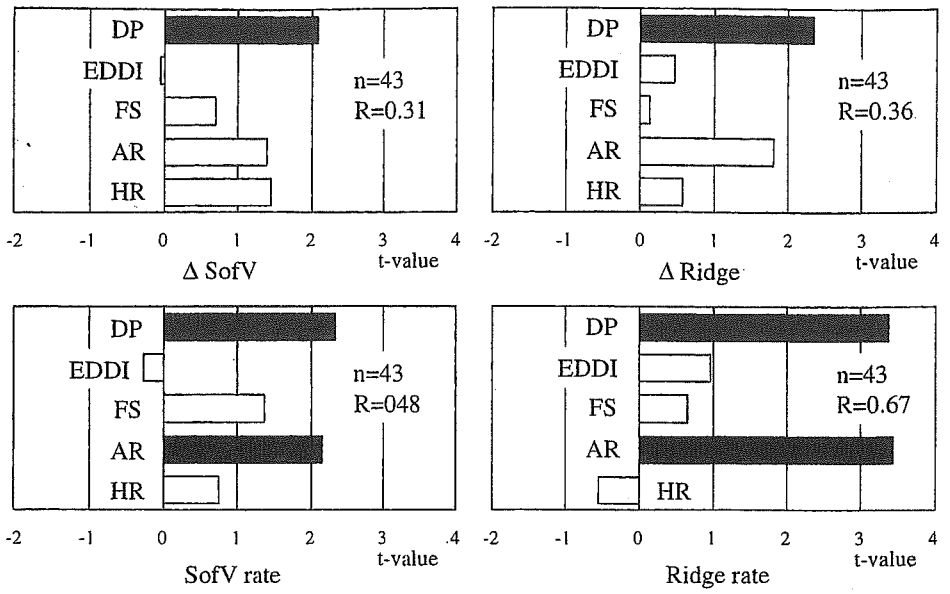

Fig. 3. Impact of patients' characteristics on annual change of aortic root diameter and on change of the aortic ratio; t values of each parameter are shown in bar graphs. Black bars indicate $P<0.05$ and white bars indicate $P>0.05$. R shows multiple correlation coefficient. AR=severity of aortic regurgitation; DP=diastolic blood pressure; EDDI=end-diastolic diameter index; FS=left ventricular fractional shortening; HR=heart rate; Δ ridge=change in supraaortic ridge diameter per year; ridge rate=change in supraaortic ridge ratio; Δ SofV=change in aortic sinuses of Valsalva diameter per year; SofV rate=change in aortic sinus ratio.

aortic root dilatation and subsequent aortic complications. Despite significant initial differences between groups in the prevalence and severity of aortic regurgitation, we found that LV size and systolic function were comparable between groups with rapid and slow progression. However, interestingly, abnormal LV diastolic filling pattern, indicating impaired LV relaxation, was more common in patients with rapid progression. Note that in this analysis, factors influencing Doppler filling parameters such as age, blood pressure, LV size, wall thickness, and aortic and mitral regurgitation grades were all comparable between patients with slow and rapid progression. Although there was a relatively small number of patients who had pulsed Doppler recordings, the features associated with impaired diastolic LV relaxation could predict more rapid aortic root dilatation and development of complications in select Marfan patients. Further, our findings could have a logical explanation when considering the potential abnormalities of the collagen matrix that may involve the myocardium in the Marfan syndrome [10]. The abnormalities of the extracellular connective tissue matrix in patients with the Marfan syndrome could involve heart muscle as well as aorta and heart valves, leading to ventricular diastolic dysfunction [10]. It has been speculated that defective microfibrils and elastic fibers in the cardiac cytoskeleton weaken the elastic restoring forces in the Marfan syndrome, and therefore LV relaxation is impaired [10].

4.2. Determinants of rapid aortic root dilatation

Since the Marfan patients with aortic root dilatation may have poor prognosis, it would be clinically important to predict which patients would progressively develop aortic root dilatation. Therefore, we performed multivariate analysis considering clinical and echocardiographic parameters as independent variables and changes in aortic root diameters as the dependent variables. We found that aortic regurgitation grade, diastolic blood pressure and LV size had significant influence on the rate of aortic root dilatation. This finding is in accord with the previously published study regarding the poorer prognosis (decreased long-term survival) in patients with diastolic murmur or cardiomegaly on initial physical examination [4]. The presence of aortic regurgitation or dilated LV, or both should be a sign to proceed in an aggressive manner to further treatment.

4.3. Clinical implications

Our study confirms the importance of age, high blood pressure, larger initial aortic ratio, and presence and severity of aortic regurgitation, abnormal Doppler diastolic filling pattern at baseline as markers of high risk of rapid progression of aortic dilatation and subsequent aortic complications. This underscores the need for more frequent control and aggressive treatment in the Marfan patients with these features.

Diastolic dysfunction has been known to precede systolic dysfunction in some forms of heart failure. We found that even in patients with rapid progression of aortic dilatation (which could represent more severe disease expression) systolic function was preserved. It appears that in the Marfan syndrome, diastolic dysfunction precedes systolic dysfunction. It may be possible that our findings, indicating impaired relaxation, may show an overture to rapid progression of aortic dilatation and the risk for aortic complications in select Marfan patients.

4.4. Study limitations

In this retrospective study, some patients had suboptimal echocardiographic recordings for measurements of aortic diameters (at supraaortic ridge and ascending aorta level) and these measurements were not included in the analysis. Furthermore, although all study patients had color Doppler recordings, only 63% of all patients had pulsed Doppler recordings. Despite of the small number of patients, the difference in LV filling pattern between the 2 groups was very prominent and consistent.

Although transmitral flow velocity pattern provides a measure of diastolic filling, almost all of the indexes derived from the pattern are load dependent [19]. Again, note that in this study LV size, wall thickness, blood pressure, and the severity of aortic regurgitation and mitral regurgitation were comparable between the 2 patient groups in which pulsed Doppler examination was performed. Therefore, effects of loading conditions would be minor.

Since only 2 patients, both from the rapid progression group, received β-blocker therapy, effect of therapy could not be addressed in this study. To clarify the relationship between LV performance and progression of aortic root dilatation, a prospective study should be conducted with a larger number of patients.

4.5. Conclusions

Marfan patients at older age, with higher blood pressure, and with significant aortic regurgitation were at high risk of progression of aortic dilatation, with the most remarkable increase at the sinuses of Valsalva. LV systolic function appeared not to relate to the progression of aortic root dilatation. Prolonged deceleration time may relate to an increased risk for aortic complications.

References

[1] Pyeritz RE. The Marfan syndrome. In: Royce PM, Steinmann B, editors. Connective tissue and its heritable disorders: molecular, genetic, and medical aspects. New York: Wiley-Liss; 1993. p. 437–68.
[2] Mc Kusick VA. The cardiovascular aspects of Marfan's syndrome: a heritable disorder of connective tissue. Circulation 1955;11:321–42.
[3] Murdoch JL, Walker BA, Halpern BL, Kuzma JW, McKussick VA. Life expectancy and causes of death in the Marfan syndrome. N Engl J Med 1972;286:804–8.
[4] Marsalese DL, Moodie DS, Vacante M, et al. Marfan's syndrom natural history and long-term follow-up of cardiovascular involv ment. J Am Coll Cardiol 1989;14:422–8.
[5] Brown OR, DeMots H, Kloster FE, Roberts A, Menashe VD, Bea RK. Aortic root dilatation and mitral valve prolapse in Marfan syndrome: an echocardiographic study. Circulation 1975;52:651–7
[6] Come PC, Fortuin NJ, White RI, McKusick VA. Echocardiograph assessment of cardiovascular abnormalities in the Marfan syndrom comparison with clinical findings and with roentgenographic estim tion of aortic root size. Am J Med 1983;74:465–74.
[7] Bruno L, Tredici S, Mangiavacchi M, Colombo V, Mazzotta G Sirtori CR. Cardiac, skeletal, and ocular abnormalities in patients wit the Marfan's syndrome and their relatives: comparison with th cardiac abnormalities in patients with kyphoscoliosis. Br Heart J 198 51:220–30.
[8] Roman MJ, Rosen SE, Kramer-Fox R, Devereux RB. Prognosti significance of the pattern of aortic root dilatation in the Marfa syndrome. J Am Coll Cardiol 1993;22:1470–6.
[9] Hollister DW, Goodfrey M, Sakai LY, Pyeritz RE. Immuno-histologi abnormalities of the microfibrillar–fiber system in the Marfa syndrome. N Engl J Med 1990;323:152–9.
[10] Savolainen A, Nisula L, Keto P, et al. Left ventricular function i children with the Marfan syndrome. Eur Heart J 1994;15:625–30.
[11] Pyeritz RE, McKusick VA. The Marfan syndrome: diagnosis and management. N Engl J Med 1979;300:772–7.
[12] De Paepe A, Devereux RB, Dietz HC, Hennekam RCM, Pyeritz RE Revised diagnostic criteria for the Marfan syndrome. Am J Med Gene 1996;62:417–26.
[13] Roman MJ, Devereux RB, Kramer-Fox R, O'Loughlin J. Two-dimensional echocardiographic aortic root dimensions in normal children and adults. Am J Cardiol 1989;64:507–12.
[14] Perry GJ, Helmcke F, Nanda NC, Byard C, Soto B. Evaluation of aortic insufficiency by Doppler color flow mapping. J Am Coll Cardiol 1987;9:952–9.
[15] Miyatake K, Izumi S, Okamoto M, et al. Semiquantiatative grading of severity of mitral regurgitation by real-time two-dimensional Doppler flow imaging technique. J Am Coll Cardiol 1986;7:82–8.
[16] Helmcke F, Nanda NC, Hsiung MC, et al. Color Doppler assessment of mitral regurgitation with orthogonal planes. Circulation 1987;75: 175–83.
[17] Levine RA, Stathogiannis E, Newell JB, Harrigan P, Weyman AG. Reconsideration of echocardiographic standards for mitral valve prolapse: lack of association between leaflet displacement isolated to the apical 4-chamber view and independent echocardiographic evidence of abnormality. J Am Coll Cardiol 1988;11:1010–9.
[18] Sahn DJ, DeMaria AN, Kisslo J, Weyman A. Recommendations regarding quantitation in M-mode echocardiography: results of a survey of echocardiographic measurements. Circulation 1978;58: 1072–83.
[19] Thomas JD, Weyman AE. Echo-Doppler evaluation of left ventricular diastolic function: physics and physiology. Circulation 1991; 84:977–90.

ELSEVIER

Atherosclerosis 185 (2006) 165–172

ATHEROSCLEROSIS

www.elsevier.com/locate/atherosclerosis

Altered expression balance of matrix metalloproteinases and their inhibitors in human carotid plaque disruption: Results of quantitative tissue analysis using real-time RT-PCR method

Takeo Higashikata[a], Masakazu Yamagishi[a,*], Toshio Higashi[b], Izumi Nagata[b], Koji Iihara[b], Susumu Miyamoto[b], Hatsue Ishibashi-Ueda[c], Noritoshi Nagaya[d], Takashi Iwase[d], Hitonobu Tomoike[a], Aiji Sakamoto[e]

[a] *Division of Cardiovascular Medicine and Bioscience, National Cardiovascular Center and Research Institute, 5-7-1 Fujishiro-dai, Suita, Osaka 565-8565, Japan*

[b] *Division of Neurosurgery, National Cardiovascular Center, Suita, Osaka, Japan*

[c] *Division of Pathology, National Cardiovascular Center, Suita, Osaka, Japan*

[d] *Division of Regenerative Medicine and Tissue Engineering, National Cardiovascular Center and Research Institute, Suita, Osaka, Japan*

[e] *Division of Biotechnology and Bioscience, National Cardiovascular Center and Research Institute, Suita, Osaka, Japan*

Received 28 October 2004; received in revised form 17 May 2005; accepted 27 May 2005
Available online 21 July 2005

Abstract

Background: The balance between degradation and synthesis of extracellular matrix determines its content in atherosclerotic tissue. To examine the role of expression balance of matrix metalloproteinases (MMPs) to their inhibitors, tissue inhibitors of metalloproteinases (TIMPs) and tissue factor pathway inhibitor-2 (TFPI-2) in the development and disruption of atherosclerotic plaque, these gene expressions in human carotid plaque were quantitatively determined by real-time reverse transcription (RT)-polymerase chain reaction (PCR) method.
Methods: Total RNA for cDNA synthesis was extracted from tissues in 24 patients with carotid endarterectomy. The amounts of cDNAs for MMP-1, -2, -3 and -9, TFPI-2 and TIMP-1, -2 and -3 were determined by real-time RT-PCR method, and normalized with glutaraldehyde 3-dehydrogenase.
Results: In plaques, the expression MMP-1 (1.53 ± 0.25, mean ± S.E.M.), MMP-3 (1.99 ± 0.59) and MMP-9 (2.00 ± 0.51) was augmented compared to those in the adjacent control regions (0.60 ± 0.16, 0.46 ± 0.18 and 0.58 ± 0.21, respectively, $p < 0.05$). The expression of TFPI-2 was lower in plaques (0.32 ± 0.08) than in controls (0.94 ± 0.23, $p < 0.01$). Although the expression of TIMP-1 was higher in plaques (1.28 ± 0.23) than in controls (0.81 ± 0.10, $p < 0.05$), the indices of MMP-1/TIMP-1, MMP-3/TIMP-3 and MMP-9/TIMP-1 were still signi. cantly higher in plaques. Interestingly, MMP-9 and the resulting MMP-9/TIMP-1 balance in plaques with disruption were signi. cantly higher (3.36 ± 1.52 and 1.66 ± 0.12, $n = 11$) than those in non-disrupted plaques (1.11 ± 0.52 and 0.76 ± 0.12, $n = 13$, $p < 0.05$).
Conclusion: With the decreased expression of TFPI-2, upregulation of MMPs in atherosclerotic plaque was disproportional to that of TIMPs, suggesting that imbalanced degradation and synthesis of extracellular matrix persists in advanced lesions, particularly in plaques with disruption.
© 2005 Elsevier Ireland Ltd. All rights reserved.

Keywords: Atherosclerosis; Extracellular matrix; Matrix metalloproteinases; Tissue inhibitor of metalloproteinases; Tissue factor pathway inhibitor-2; Plaque disruption

1. Introduction

Disruption of atherosclerotic plaque during its development can expose the thrombogenic core to luminal blood . ow, frequently resulting in ischemic cardiac events and stroke

* Corresponding author. Tel.: +81 6 6833 5012; fax: +81 6 6833 9865.
E-mail address: myamagi@hsp.ncvc.go.jp (M. Yamagishi).

0021-9150/$ – see front matter © 2005 Elsevier Ireland Ltd. All rights reserved.
doi:10.1016/j.atherosclerosis.2005.05.039

[1,2]. During this process, structural changes in extracellular matrix (ECM) were shown to play a crucial role in plaque development and disruption [3]. The structural integrity of plaques seems to depend on a balance between synthesis and degradation of the ECM which is mainly regulated by proteinases such as matrix metalloproteinases (MMPs) including interstitial collagenase or MMP-1, gelatinase A or MMP-2, stromelysin 1 or MMP-3, gelatinase B or MMP-9 [4,5].

The activities of MMPs are controlled on multiple levels: transcription and translation of their inactive precursors (zymogens), post-translational activation of zymogens by proteolysis and interactions with tissue inhibitors of metalloproteinases (TIMPs) [6] and/or tissue factor pathway inhibitor-2 (TFPI-2) [7]. Indeed, TIMPs-1, -2, -3 and TFPI-2 are expressed in atherosclerotic lesions [7–9], and these inhibitors bind to and inactivate most of the MMPs [7,10]. Thus, the expression balance of MMP to TIMP and TFPI-2 is considered to regulate the net degeneration of ECM, thus contributing to maintaining plaque stability [7,11,12]. However, few systematic data exist regarding quantitative evaluation of the expression of MMPs and their inhibitors in human atherosclerotic plaques, probably because of technical dif. culties in simultaneous determination of multiple gene expression in small tissue samples obtained in clinical settings. In the present study, we used real-time reverse transcription (RT)-polymerase chain reaction (PCR) and analyzed gene expression levels of MMPs, TIMPs and TFPI-2 in human carotid plaque and an adjacent control region. We also compared expression and function of MMPs between histologically disrupted and non-disrupted plaques.

2. Subjects and methods

2.1. Subjects

The protocol of this study was approved by the institutional committee for ethical review. Written informed consent was obtained from all 24 patients who underwent carotid endarterectomy for severe stenosis of the extracranial carotid artery (all male with mean age of 68 ± 2 years). All patients presented clinical symptoms of cerebral ischemic attack related to carotid stenosis. Seven patients had a history of recent ischemic attack within 1 month prior to endarterectomy. The prevalence of risk factors for atherosclerosis was as follows: hypertension (systolic pressure >160 mmHg) in 20, hyperlipidemia (total cholesterol >220 mg/dl) in 22, smoking in 15 and diabetes mellitus (fasting blood glucose >110 mg/dl) in 10 patients. High sensitive (hs) CRP level (normal range <3 mg/l) just before surgery was 2.45 ± 0.43 mg/l (Table 1).

2.2. Tissue sampling

Samples of the plaque region were obtained immediately after endarterectomy. Endarterectomy was extended in a caudal direction to include a sample of minimally affected common carotid artery proximal to the plaque but in continuity with the plaque to act as a paired control. Under these conditions, the stenotic segment and adjacent areas were dissected undisruptedly as a single specimen, preserving circumferential integrity as much as possible. Also special care was taken not to damage luminal surface and plaque interior. After removing a part of the tissue for histological examination, all samples were immediately frozen in liquid nitrogen and stored at −80 °C until extraction of mRNA.

Procedures for RNA preparation and cDNA synthesis were already described elsewhere in detail [13]. Brie. y, the samples were homogenized in 1.0 ml ISOGEN™ reagent (Nippon Gene, Tokyo, Japan), thoroughly mixed with 0.2 ml chloroform and centrifuged at 15,000 × *g* for 15 min at 4 °C. The aqueous supernatant was transferred into a micro test tube, mixed with 0.6 ml isopropanol and centrifuged at 15,000 × *g* for 15 min at 4 °C. The precipitated total RNA was rinsed with 70% ethanol, air-dried and then resuspended in RNase-free water. Then, all the total RNA was treated with DNase Free™ reagent (Ambion, Austin, TX) for 60 min, and then reverse-transcribed with Superscript II™ (Invitrogen, Carlsbad, CA) at 37 °C for 60 min using random primers (TaKaRa, Tokyo, Japan). The integrity of each cDNA mixture was checked by ampli. cation of glutaraldehyde 3-phosphate dehydrogenase (GAPDH) with *ExTaq* (TaKaRa), using the primer set 5′-ACCACAGTCCATGCCATCAC-3′/5′-TCCACCACCCTGTTGCTGTA-3′.

Table 1
Patient Characteristics

	All patients (n = 24)	With disruption (n = 11)	Without disruption (n = 13)	p-Value
Age	68 ± 2	66 ± 3	69 ± 2	NS
Male sex	24	11	13	NS
Hypertension	20	8	12	NS
Diabetes	10	5	5	NS
HbA1c (%)	6.5 ± 0.4	7.0 ± 0.8	6.2 ± 0.4	NS
Hyperlipidemia	22	9	13	NS
LDL (mg/dl)	132 ± 6	140 ± 10	128 ± 7	NS
Smoking	15	5	10	NS
hs-CRP (mg/l)	2.45 ± 0.43	2.68 ± 0.49	2.12 ± 0.81	NS

2.3. Primers and probes for real-time RT-PCR

Using Primer Express™ software (Applied Biosystems, Foster, CA), primers were designed for each of the genes for MMP-1, -2, -3 and -9, TFPI-2 and TIMP-1, -2 and -3, and the TaqMan probe inherent to each primer set was prepared, which was an oligonucleotide labeled with a reporter dye (FAM) at the 5′-end and a quencher dye (TAMRA) at the 3′-end. The sequences of the primers and TaqMan probes of MMPs-1, -2, -3, -9, TIMPs-1, -2 and -9 were reported elsewhere [13], and those for TFPI-2 were SENSE = CGATGCTTGCTGGAGGATAGA; ANTISENSE = ACACTGGTCGTCCACACTCACT; Taqman probe = 5′-FAM-AAGTTCCCAAAGTTTGCCGGCTGC-TAMRA-3′; TFPI-2 SENSE = CGATGCTTGCTGGAGGATAGA; ANTISENSE = ACACTGGTCGTCCACACTCACT; Taqman probe = 5′-FAM-AAGTTCCCAAAGTTTGCCGGCTGC-TAMRA-3′.

Real-time RT-PCR was performed using an ABI PRISM 7700 Sequence Detection System (Applied Biosystems). The reaction solution was assembled in a volume of 25 μl, which comprised TaqMan Universal PCR Master Mix (Applied Biosystems), forward and reverse primers (. nal concentration 300 nM each), TaqMan probe (. nal concentration 200 nM) and cDNA mixture (about 2.5 ng). Throughout this study, the cDNA mixture from a particular sample was used to generate the working standard for quantitation of the cDNA of interest, which plots the relationship between the dilution of the standard cDNAs and the corresponding C_t value (the number of cycles necessary to obtain a threshold . uorescent signal) [13]. The initial quantity of the cDNA of interest in a certain cDNA mixture was calculated from the working standard and then normalized to that of GAPDH determined with TaqMan Assay Reagent Endogenous Control™ (Applied Biosystems). The normalized value for each target cDNA re. ects the expression level of the corresponding gene in a test sample relative to the standard tissue. The accuracy of the present real-time RT-PCR for determining mRNA expression in human vascular tissue was already con. rmed by comparing the results with those determined by conventional RT-PCR method [13].

2.4. Expression and function of MMP

To determine expression and function of MMP in its protein level, carotid tissue samples from 10 patients, in whom enough amounts of proteins could be extracted, were examined by Western blotting and gel zymography. The extracted protein was separated by SDS-PAGE and blotted onto a Hybond-ECL nitrocellulose membrane (Amersham) with the use of primary (40 μg/ml) and secondary (1:2000, Amersham) antibodies. As for zymography, proteins with gelatinolytic activity were identi. ed by use of substrate gels prepared by incorporation of gelatin (1 mg/ml; Wako) into a SDS-PAGE. After elecrophoresis, gels were washed in 2.5% Triton X-100 for 30 min to remove SDS. The gel was equilibrated for 30 min at room temperature with gentle agitation then incubated for overnight at 37 °C in 50 mM Tris/HCl, pH 7.5, containing 0.2 M NaCl, 5 mM $CaCl_2$ and 0.02% Brij 35. Gels were then . xed and stained with 0.25% Coomassie Brilliant Blue R-250 (Wako). The product of the optical net density of the band was compared with a positive control (HT-1080 human . brosarcoma cells for Western blotting and human MMP-2 and human MMP-9, 1.5 ng, CC073; CHEMICON for zymography) to obtain a ratio comparable between gels.

2.5. Histology and immunohistochemistry

A part of the plaque was placed in tissue . xative (Histochoice, Hedwin, Baltimore). After overnight . xation, the samples were paraf. n embedded and sectioned at 4-μm intervals. Tissue sections were deparaf. nized with xylene followed by immersion in graded alcohol. They were washed three times for 5 min each in phosphate-buffered saline (PBS) and blocked with bovine serum albumin for 60 min. Specimens were then incubated with primary antibodies against CD-68, MMPs, TIMPs and TFPI-2 (Fuji Chemical, Tokyo, Japan) overnight at 4 °C. After they were washed in PBS, specimens were incubated with biotinylated rabbit anti-mouse IgG for 60 min at room temperature. Specimens were then washed with PBS, stained with horseradish peroxidase-conjugated streptavidin, and . nally incubated with substrate solution for 1–15 min. The tissue sections were also stained with hematoxylin–eosin and elastica van Gieson for evaluation of plaque composition and . brous cap disruption, as described by Carr et al. [2]. Plaque was de. ned as atheromatous if the area of lipid core was ≥30% of the whole plaque area and as . brous plaque if <30% in terms of its vulnerability [14].

2.6. Data analysis

The mean and standard error of triplicate data are presented. Statistical analysis was performed by paired *t*-test using Stat View 5.0 software on a Macintosh computer and by Wilcoxon matched-pair signed-rank test if appropriate. A *p*-value <0.05 was considered signi. cant.

3. Results

3.1. Patient and plaque characteristics

Atheromatous plaque was observed in 15 samples and . brous plaque in 9 samples. Disruption of the . brous cap was observed in 11 samples with atheromatous plaque and was not observed in 13 samples, which consisted of 4 atheromatous and 9 . brous plaques. Although levels of HbA1c and LDL-cholesterol in patients with plaque disruption tended to be higher than those in patients without disruption, there was no statistically signi. cant difference in their clinical back-

Table 2
MMP, TFPI-2 and TIMP levels

Mrna	Control	Plaque	p-Value
MMP-1	0.60 ± 0.16	1.53 ± 0.25	<0.01
MMP-2	0.80 ± 0.11	0.88 ± 0.14	NS
MMP-3	0.46 ± 0.18	1.99 ± 0.59	<0.05
MMP-9	0.58 ± 0.21	2.00 ± 0.51	<0.01
TFPI-2	0.94 ± 0.23	0.32 ± 0.08	<0.01
TIMP-1	0.81 ± 0.10	1.28 ± 0.23	<0.05
TIMP-2	1.12 ± 0.15	0.95 ± 0.17	NS
TIMP-3	0.47 ± 0.16	0.67 ± 0.17	NS

ground. Also there was no difference in hs-CRP level between two patient groups, although mean value in all patients was higher than normal value (Table 1).

3.2. Expression levels of MMPs, TIMPs and TFPI-2

From removed samples with a wet weight of 11.69 ± 2.64 mg, 0.49 ± 0.22 μg total RNA was extracted for analysis. Ampli. cation of GAPDH was equivalent among all the cDNAs synthesized. Each primer set for PCR exponentially ampli. ed its target cDNA according to the cycle number. Normalized values for MMP, TIMP and TFPI-2 gene expression in plaque and adjacent control tissue (controls) are summarized in Table 2. In the plaques, the gene expression levels of MMP-1 (1.53 ± 0.25), MMP-3 (1.99 ± 0.59) and MMP-9 (2.00 ± 0.51) were signi. cantly higher than those in the controls (0.60 ± 0.16, 0.46 ± 0.18 and 0.58 ± 0.21, respectively, $p < 0.05$). However, no difference was found in the expression level of MMP-2 gene between the plaques and controls (0.88 ± 0.14 versus 0.80 ± 0.11). It was quite interesting that TFPI-2 gene expression was signi. cantly higher in the controls (0.94 ± 0.23) than that in plaques (0.32 ± 0.08, $p < 0.01$).

As for TIMP genes, the only TIMP-1 gene was signi. - cantly upregulated in plaques in comparison with that in the controls (1.28 ± 0.23 versus 0.81 ± 0.10, $p < 0.05$) (Table 2). Among the combination of the ratios of the four MMPs to the three TIMPs examined in this study, the expression ratios of MMP-1 to TIMP-1, MMP-3 to TIMP-3 and MMP-9 to TIMP-1 were signi. cantly higher in plaques than in the controls (2.98 ± 0.77 versus 0.99 ± 0.43, 2.18 ± 0.53 versus 0.63 ± 0.22 and 1.80 ± 0.14 versus 0.83 ± 0.09, respectively, $p < 0.05$) (Fig. 1). Of interest, in plaques with disruption of . brous cap, MMP-9 expression (3.36 ± 1.52) and the ratio of MMP-9 to TIMP-1 (1.66 ± 0.12) were signi. cantly higher than those in plaques without disruption (1.11 ± 0.52 and 0.76 ± 0.12, respectively), although TFPI-2 gene expression was not different between these groups (0.27 ± 0.08 versus 0.40 ± 0.18).

MMP-9 protein was expressed both in disrupted and non-disrupted plaques, but was not expressed or only slightly expressed in controls. Under these conditions, net expression of MMP-9 was signi. cantly higher in disrupted (2.61 ± 0.17,

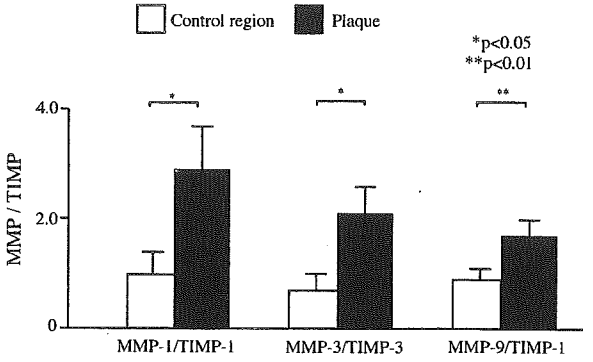

Fig. 1. Imbalanced expression of matrix metalloproteinase (MMP) to tissue inhibitor of matrix metalloproteinase (TIMP) genes in carotid plaque. Vertical axis represented the ratio of MMP/TIMP. Open columns represent values from control regions and closed columns values from plaques.

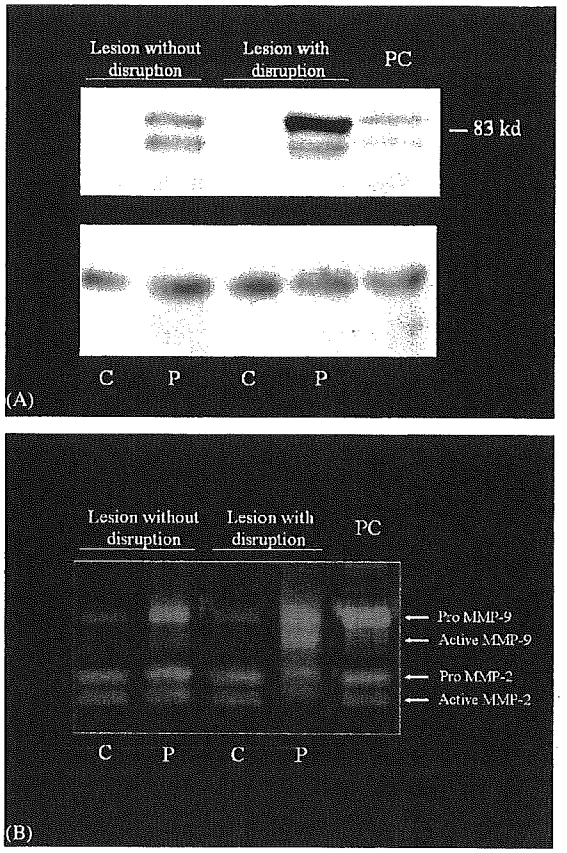

Fig. 2. Expression and function of MMP-9 in protein level. (A) Western blotting for matrix metalloproteinase MMP-9 (upper) and an internal marker protein, endothelin receptor (ETR) (lower), in non-ruptured lesion, ruptured carotid lesions and positive control (PC). MMP-9 was clearly expressed in the plaque (P) and PC, whereas in the control region (C), little expression of MMP-9 was observed. Note that both pro* and active** form of MMP-9 appears to be highly expressed in the ruptured plaque, in comparison with the non-ruptured plaque, although ETR protein is equally expressed. (B) By zymography, increased size and staining of both pro- and active forms of MMP-9 particularly in ruptured plaques, although MMP-2 activity was not different in each lane as observed in mRNA analysis.

$n=4$) than in non-disrupted plaques (1.11 ± 0.12, $n=6$, $p<0.05$), despite the equal expression of an internal marker protein, endothelin-1 receptor (Fig. 2A). Interestingly, the amount of active form MMP-9 determined by zymography was signi. cantly higher in the disrupted (2.62 ± 0.12) than in non-disrupted plaques (0.72 ± 0.07, $p<0.05$), although pro MMP-9 activity was not signi. cantly different in disrupted (1.8 ± 0.10) and non-disrupted plaques (1.4 ± 0.11) (Fig. 2B). There were no signi. cant differences between the levels of pro and active forms of MMP-2, as demonstrated in its mRNA expression.

3.3. Immunohistochemistry

In the adjacent control regions (Fig. 3A), there was mild atherosclerosis where a few CD-68 positive macrophages existed. Under these conditions, MMPs and TIMPs were scatteringly positive. In contrast, TFPI-2 was diffusely positive in the intima and media. Plaque regions mainly consisted of lipid-rich core and . brous tissue (Fig. 3B) where CD-68 positive macrophages were accumulated particularly in the shoulder regions of atheroma and all MMPs and TIMPs were strongly positive. It was interesting that, under these conditions, TFPI-2 was regionally positive in the plaque regions. Because of small number of examined plaques, we could not correlate expression of MMPs, TIMPs and TFPI-2 to the stage of plaque development.

4. Discussion

4.1. Gene expression of MMPs, TIMPs and TFPI-2 in plaque

One of the striking . ndings of the present study was that with a decreased TFPI-2 gene expression, the MMP-9 gene together with the MMP-9 protein was signi. cantly upregulated in plaques, particularly in plaques with disrupted . brous cap. Increased production of MMP-9 is thought to contribute to the progressive deterioration of the elastic lamellae associated with vessel remodeling, which could be closely related to the occurrence of plaque disruption [15]. Indeed, previous studies indicated that MMP-9 was present in the coronary plaque from unstable angina [16] and carotid plaque from

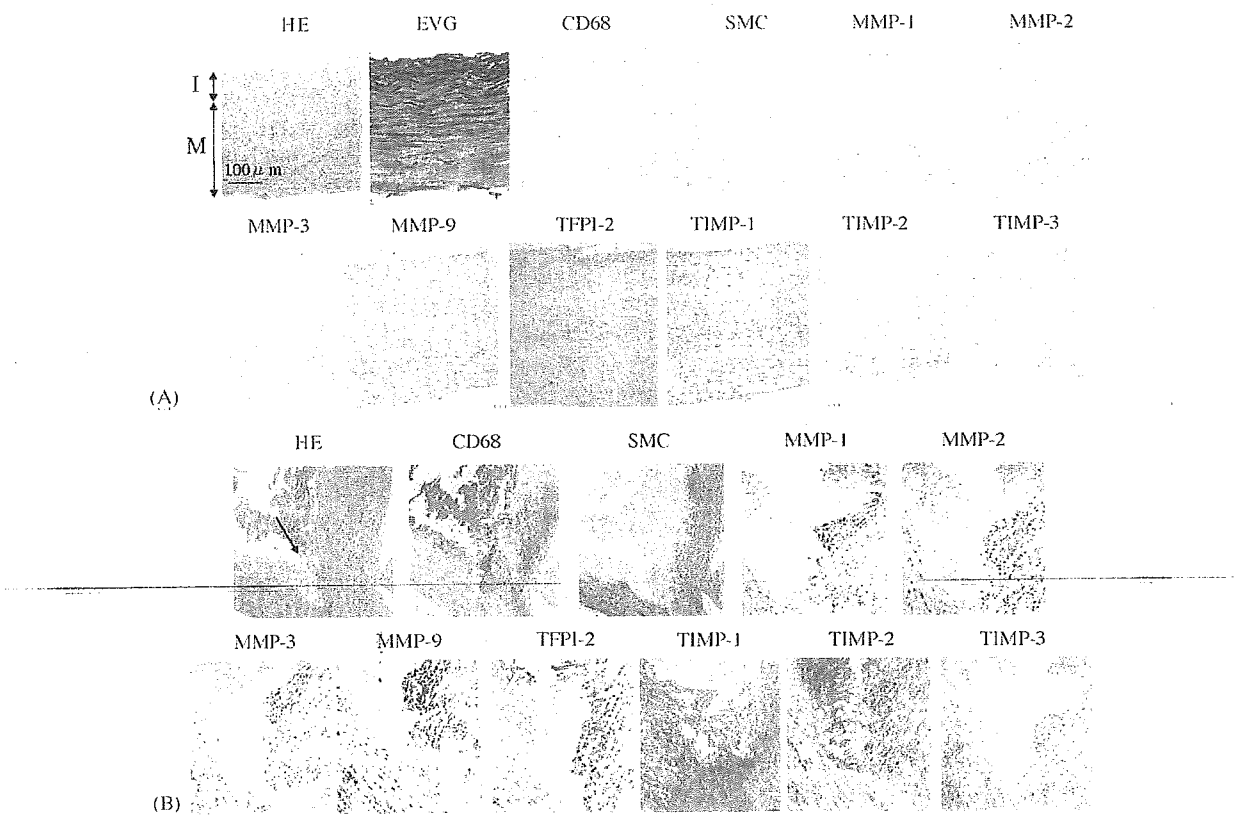

Fig. 3. Histologic and immunohistologic . ndings (with original magni. cation of ×25). (A) In the control tissues, there existed mild atherosclerotic lesion where a few CD-68 positive macrophages was found. Under these conditions, tissue factor pathway inhibitor (TFPI)-2 was diffusely positive in the intima and media, although matrix metalloproteinases (MMPs) and tissue inhibitor of MMPs (TIMPs) were scatteringly positive. An arrow indicates boundary between intima and media. (B) In plaque lesions with a lipid-rich core where CD-68 positive macrophages were accumulated, all MMPs and TIMPs were strongly positive particularly in the shoulder regions of atheroma (arrow). It was interesting that, under these conditions, TFPI-2 was regionally positive in this lesion. EVG, elastica van Gieson; HE, hematoxylin–eosin; I, intima; M, media; SMC, smooth muscle cell.

symptomatic patients [17]. We in fact demonstrated greater upregulation and function of MMP-9 in plaques with . ssured . brous cap at the mRNA as well as protein level, based on histological . ndings.

Simultaneous upregulation of the MMP-1 and -3 genes was also observed, as previously reported [18,19]. MMP-1 speci. cally cleaves collagen types I and III, which are key components of the extracellular framework of the arterial wall and major constituents of human atherosclerotic plaques, and activate other MMPs [6] that degrade denatured collagen, gelatin and elastin. MMP-3 has the widest substrate repertoire of all MMPs, showing activity against most of the extracellular proteins and proteoglycans [20]. However, unlike MMP-9, there were no differences in the expression of MMP-1 and -3 genes between plaques with and without rupture. This suggests that simultaneous upregulation of these MMPs is a plausible phenomenon in the development of atherosclerotic plaques.

This study demonstrates diminished gene expression of TFPI-2 in plaques that contain abundant MMPs. TFPI-2, originally considered as a serine proteinase inhibitor, is known to be highly expressed in smooth muscle cells of the relatively non-diseased tissue favoring ECM stability by inactivating collagenases such as MMP-1 as well as gelatinases probably through direct protein/protein interactions. Indeed, Herman et al. [7] demonstrate inverse relation between TFPI and MMP activity in atherosclerotic tissue. Thus, decreased TFPI-2 gene expression in plaques, as observed in the present study, might allow increased matrix degradation by MMP-1, -3 and -9 in plaques, enhancing their susceptibility to plaque development. It is interesting, under these conditions, TIMP-1 exhibited signi. cantly higher expression in plaques than in controls. The combined deletion of TIMP-1 and ApoE in mice leads to a reduction in atherosclerotic plaque size [21], whereas overexpression of TIMP-1 induced by adenovirus-mediated transfer in ApoE-de. cient mice leads to a decrease in plaque size and an increase in collagen content [22]. Taken together, under the condition where TFPI-2 was diminished to express, upregulation of TIMP-1 seems to counteract overexpression of MMPs, to exert an inhibitory effect on the development of atherosclerotic plaque.

However, the expression ratios of MMPs to TIMP-1 were still higher in the plaque compared with the control regions. Compensatory expression of TIMP-1 might not be suf. - cient to counteract the degenerative role of MMPs in the plaque, thus contributing to the development of atherosclerotic plaque. Particularly, the MMP-9/TIMP-1 ratio was signi. cantly higher in plaques with disruption than in those without disruption. This suggests the functional signi. cance of the imbalance of expression of these genes in the occurrence of plaque disruption. It would be of interest to examine which can play a more important role, TFPI-2 or TIMP-1, for the regulation of MMP activity, since compartmentalization might result in distinct microenvironments with corresponding variations in MMP/inhibitor ratios.

4.2. Clinical implications and limitations

A recent experimental study in which local MMP-9 was upregulated by gene transfection resulted in enhanced formation of local thrombus [23]. On the contrary, manipulation to augment expression of expression of TIMPs prevented the occurrence of plaque disruption [22]. Therefore, one might speculate that the altered balance of MMP-9/TIMP-1 with decreased TFPI-2 observed in the present study contributes to plaque disruption associated with or without regional thrombosis.

The carotid plaques examined in the present study were obtained from highly stenotic lesion probably representing the . nal stage of plaque development and destabilization. In acute coronary syndrome, however, atherosclerotic plaque disruption is known to occur at the sites of mild to moderate stenotic lesions [24] that were not examined in the present study. Although preliminary results indicate that in coronary plaques related to acute coronary syndrome MMP-9 gene was highly expressed in comparison with that in plaques from stable coronary disease [25], further study will need to con- . rm gene expression in carotid plaque from mild to moderate stenotic lesion.

The present study has a limitation regarding histological assessment of the presence of plaque disruption. Only a small portion of each plaque was examined histologically, and it may well be that features were missed in some patients. Several reports suggest that vulnerability to plaque rupture is a multifocal phenomenon particularly at the time of acute presentation [26,27]. Conversely, one might argue that we did not necessarily determine mRNA expression levels in the part of the plaque where histological analysis was performed. Even under these conditions, imbalanced expression of MMPs/TIMPs with reduction of TFPI-2 was observed in plaques, particularly in those associated with disruption. That the control regions were obtained from adjacent to the culprit lesion is another limitation. However, there was no histological evidence for plaque disruption in the control regions used for present study even in the presence of mild atherosclerosis. It can not be excluded, however, that the disruption of the . brous cap could be resulted from surgical procedure, although we carefully examined the part of plaque where surgical procedures was not affected.

Whether upregulation of MMPs is the cause or result of plaque disarrangement is unclear. A recent study suggested that MMP-9 might have a protective effect against plaque development in double ApoE and MMP-9 knockout mice [28]. Thus, a causal relationship cannot be concluded until a controlled trial with a speci. c MMP-9 inhibitor is performed. Recently, MMP-8, traditionally associated only with neutrophils, which enhanced matrix breakdown by activating MMPs and/or by inactivating TIMP-1, was found to be highly expressed in macrophages in disrupted plaques [29]. Reduced expression of TFPI-2 might be related to the enhanced expression of neutrophil elastase in plaques, although MMP-

8 gene expression was not determined in the present study.

In the present study, we used real-time RT-PCR, which gives an estimate of mRNA expression instead of protein level for each enzyme and inhibitor, because it is still dif. cult to extract some proteases such as MMP-1, which binds strongly to connective tissue and to quantitatively assay enzyme activities [30]. However, it is important to determine the activity of TIMPs in protein level, since determination of gene expression can sometimes misinterpret the actual change of protein expression [31]. Therefore, evaluation of mRNA expression of multiple genes by the present real-time RT-PCR method in combination with determination of protein should be done for systematic evaluation of the activities of MMPs, TIMPs and TFPI-2 in clinical tissue samples.

Finally, the precise mechanism of the sustained overexpression of MMPs and TIMPs with reduction of TFPI-2 in advanced atherosclerotic plaque is still unclear. Our preliminarily report indicate that CXCR-2, a chemokine receptor, gene was highly upregulated in accordance with MMP expression in macrophages [32]. This suggests that overexpression of MMPs could be related to a continuous in. ammatory reaction, although there was no difference in serum levels of hs-CRP between patients with ruptured and non-ruptured plaques. Further study of the regulatory mechanisms of chemokine and cytokine systems with transcription factors that also play a crucial role in MMP expression [33] may demonstrate a signi. cant pathway for the expression and activation of proteinases and their inhibitors in human atherosclerotic lesions.

5. Conclusion

We applied a real-time RT-PCR method to quantitate mRNA expression in small samples of human carotid plaque. Levels of MMP-1, -3, -9 and TIMP-1 mRNAs were significantly upregulated in human carotid plaque where TFPI-2 mRNA was decreased to be expressed. The particular upregulation of MMP-9 and resultant imbalance of MMP-9/TIMP-1 expression could play a pivotal role in plaque disruption.

Acknowledgements

This work was supported in part by grants from the Ministry of Health, Welfare and Labor of Japan and from the Cardiovascular Research Foundation (to M.Y.), the Promotion of Fundamental Studies in Health Science of the Organization for Pharmaceutical Safety and Research (OPSR) of Japan (to A.S.), and the Japan Cardiovascular Research Foundation (to A.S.). A part of this work was presented at the 53rd Annual Scienti. c Session, American College of Cardiology, in New Orleans, 2004.

References

[1] Falk E, Shah PK, Fuster V. Coronary plaque disruption. Circulation 1995;92:657–71.
[2] Carr S, Farb A, Pearce WH, et al. Atherosclerotic plaque rupture in symptomatic carotid artery stenosis. J Vasc Surg 1996;23:755–65.
[3] Libby P. In. ammation in atherosclerosis. Nature 2002;420:868–74.
[4] Dollery CM, McEwan JR, Henney AM. Matrix metalloproteinases and cardiovascular disease. Circ Res 1995;77:863–8.
[5] Galis ZS, Khatri JJ. Matrix metalloproteinases in vascular remodeling and atherogenesis: the good, the bad, and the ugly. Circ Res 2002;90:251–62.
[6] Nagase H. Activation mechanisms of matrix metalloproteinases. Biol Chem 1997;378:151–60.
[7] Herman MP, Sukhova GK, Kisiel W, et al. Tissue factor pathway inhibitor-2 is a novel inhibitor of matrix metalloproteinases with implications for atherosclerosis. J Clin Invest 2001;107:1117–26.
[8] Fabunmi RP, Sukhova GK, Sugiyama S, et al. Expression of tissue inhibitor of metalloproteinases-3 in human atheroma and regulation in lesion-associated cells: a potential protective mechanism in plaque stability. Circ Res 1998;83:270–8.
[9] Galis ZS, Sukhova GK, Lark MW, et al. Increased expression of matrix metalloproteinases and matrix degrading activity in vulnerable regions of human atherosclerotic plaques. J Clin Invest 1994;94:2493–503.
[10] Brew K, Dinakarpandian D, Nagase H. Tissue inhibitors of metalloproteinases: evolution, structure and function. Biochim Biophys Acta 2000;1477:267–83.
[11] Knox JB, Sukhova GK, Whittemore AD, et al. Evidence for altered balance between matrix metalloproteinases and their inhibitors in human aortic diseases. Circulation 1997;95:205–12.
[12] Sternlicht MD, Werb Z. How matrix metalloproteinases regulate cell behavior. Annu Rev Cell Dev Biol 2001;17:463–516.
[13] Higashikata T, Yamagishi M, Sasaki H, et al. Application of real-time RT-PCR to quantifying gene expression of matrix metalloproteinases and tissue inhibitors of metalloproteinases in human abdominal aortic aneurysm. Atherosclerosis 2004;177:353–60.
[14] Kolodgie FD, Burke AP, Farb A, et al. The thin-cap . broatheroma: a type of vulnerable plaque, the major precursor lesion to acute coronary syndrome. Curr Opin Cardiol 2001;16:285–92.
[15] Schoenhagen P, Ziada KM, Kapadia SR, et al. Extent and direction of arterial remodeling in stable versus unstable coronary syndromes: an intravascular ultrasound study. Circulation 2000;101:598–603.
[16] Brwon DL, Hibbs MS, Kearney M, et al. Identi. cation of 92-kD gelatinase in human coronary atherosclerotic lesions. Association of active enzyme synthesis with unstable angina. Circulation 1995;91:2125–31.
[17] Loftus IM, Naylor AR, Goodall S, et al. Increased matrix metalloproteinase-9 activity in unstable carotid plaques. A potential role in acute plaque disruption. Stroke 2000;31:40–7.
[18] Nikkari ST, O'Brien KD, Ferguson M, et al. Intestinal collagenase (MMP-1) expression in human carotid atherosclerosis. Circulation 1995;92:1393–8.
[19] Sukhova GK, Schonbeck U, Rabkin E, et al. Evidence for increased collagenolysis by intersitial collagenases-1 and -3 in vulnerable atheromatous plaques. Circulation 1999;99:2503–9.
[20] Sato H, Takino T, Okada Y, et al. A matrix metalloproteinase expressed on the surface of invasive tumor cells. Nature 1994;370:61–5.
[21] Silence J, Collen D, Lijnen HR. Reduced atherosclerotic plaque but enhanced aneurysm formation in mice with inactivation of the tissue inhibitor of metalloproteinase-1 (TIMP-1) gene. Circ Res 2002;90:897–903.
[22] Rouis M, Adamy C, Duverger N, et al. Adenovirus-mediated overexpression of tissue inhibitor of metalloproteinase-1 reduces atherosclerotic lesions in apolipoprotein E-de. cient mice. Circulation 1999;100:533–40.

[23] Morishige K, Shimokawa H, Matsumoto Y, et al. Overexpression of matrix metalloproteinase-9 promotes intravascular thrombus formation in porcine coronary arteries in vivo. Cardiovasc Res 2003;57:572–85.
[24] Yamagishi M, Terashima M, Awano K, et al. Morphology of vulnerable coronary plaque: insights from follow-up of patients examined by intravascular ultrasound before an acute coronary syndrome. J Am Coll Cardiol 2000;35:106–11.
[25] Higo S, Nanto S, Higashikata T, et al. Impact of altered expression balance of matrix metalloproteinases and tissue inhibitor of metalloproteinases genes on coronary plaque rupture: results from quantitative tissue analysis using real-time reverse transcriptase-polymerase chain reaction method (abstr). J Am Coll Cardiol 2004;43(Suppl. A):257A.
[26] Rioufol G, Finet G, Ginon I, et al. Multiple atherosclerotic plaque rupture in acute coronary syndrome. A three-vessel intravascular ultrasound study. Circulation 2002;106:804–8.
[27] Schoenhagen P, Stone GW, Nissen SE, et al. Coronary plaque morphology and frequency of ulceration distant from culprit lesions in patients with unstable and stable presentation. Arterioscler Thromb Vasc Biol 2003;23:1895–900.
[28] Johnson J, George A, Newby C. Matrix metalloproteinase-9 and -12 have opposite effects on atherosclerotic plaque stability (abstr). Atherosclerosis 2003;4(Suppl.):196.
[29] Dollery CM, Owen CA, Sukhova GK, et al. Neutrophil elastase in human atherosclerotic plaques. Production by macrophages. Circulation 2003;107:2829–36.
[30] Woessner JR. Quanti. cation of matrix metalloproteinases in tissue samples. Methods Enzymol 1995;248:510–28.
[31] Blindt R, Vogt F, Lamby D, et al. Characterization of differential gene expression in quiescent and invasive human arterial smooth muscle cells. J Vasc Res 2002;39:340–52.
[32] Yamagishi M, Higashikata T, Higashi T, et al. Sustained upregulation of chemokine and its receptor genes associated with matrix metalloproteinase overexpression in human carotid plaque rupture: results from a quantitative study with real-time reverse transcriptase-polymerase chain reaction method (abstr). J Am Coll Cardiol 2004;43(Suppl.):497A.
[33] Chase AJ, Bond M, Crook MF, et al. Role of nuclear NF-κB activation in metalloproteinase-1 -3 and -9 secretion by human macrophages in vitro and rabbit form cells produced in vivo. Arterioscler Thromb Vasc Biol 2002;22:765–71.

Circ J 2005; **69:** 1490–1495

Sustained Upregulation of Inflammatory Chemokine and Its Receptor in Aneurysmal and Occlusive Atherosclerotic Disease

—— Results From Tissue Analysis With cDNA Macroarray and Real-Time Reverse Transcriptional Polymerase Chain Reaction Methods ——

Masakazu Yamagishi, MD; Takeo Higashikata, MD*; Hatsue Ishibashi-Ueda, MD**; Hiroaki Sasaki, MD†; Hitoshi Ogino, MD†; Koji Iihara, MD††; Susumu Miyamoto, MD††; Noritoshi Nagaya, MD‡; Hitonobu Tomoike, MD; Aiji Sakamoto, MD*

Background Although cytokines are known to be pivotal in the development of atherosclerotic diseases, few data exist regarding their expressions in the established stages such as aneurysmal or occlusive lesions. Therefore, in the present study the gene expression levels of cytokine-related substances in abdominal aortic aneurysm (AAA) and carotid artery stenosis (CAS) were determined using cDNA macroarray and real-time reverse transcriptase polymerase chain reaction (RT-PCR) methods.

Methods and Results Tissue samples were obtained from 31 patients with AAA and 24 with CAS. The array-specific [^{33}P]-labeled cDNA probe mixture synthesized from 2.5• g total RNA with gene-specific primers was hybridized with nylon membranes containing 375 cDNA clones. Densitometric analysis confirmed differences in expression (>5-fold) for 97 of the cytokine-related gene products between AAA and adjacent control tissue. Among these, simultaneous upregulation was found in the expression of interleukin (IL)-8 (9-fold) and its receptor, CXCR-2 (11-fold). Thus, the expressions of IL-8 and CXCR-2 were further quantified by real-time RT-PCR. The expression of both the genes was significantly upregulated in both AAA and CAS compared with control regions as followed: IL-8=0.53±0.16 vs 0.11±0.04 ($p<0.01$); CXCR-2=2.04±0.75 vs 0.29±0.10 ($p<0.01$) in AAA, and IL-8=1.35±0.25 vs 0.60±0.16; CXCR-2=2.00±0.51 vs 0.58±0.21 ($p<0.05$) in CAS. Under these conditions, the gene expressions of monocyte chemotactic protein-1 and its receptor, CCR-2, were not significantly different in the control and diseased regions of both AAA and CAS.

Conclusions Sustained upregulation of IL-8 and CXCR-2 was observed in both AAA and CAS, suggesting the inflammatory process is still active in established dilated and occlusive atherosclerotic diseases. Whether upregulation of this system could be protective or not protective for disease development requires further study. (*Circ J* 2005; **69:** 1490–1495)

Key Words: Aneurysm; Atherosclerosis; CCR-2; Chemokines; CXCR-2; Interleukin-8

Upregulation of several genes relevant to the pathophysiology of dilated atherosclerotic diseases, such as abdominal aortic aneurysm (AAA), and stenotic diseases, such as carotid artery stenosis (CAS), has been demonstrated, particularly regarding enzymes of the matrix metalloproteinase (MMP) family and their endogenous inhibitors.[1] Indeed, we previously reported that in both AAA and CAS of human tissues, upregulation of MMP genes was observed in comparison with adjacent control tissues.[2,3]

In the early stage of atherosclerosis, cytokines such as monocyte chemotactic protein (MCP)-1, interleukin (IL)-6 and their receptors are overexpressed, which contributes to the initiation and development of atherosclerotic disease.[4–6] However, for the established stage of these diseases when the clinical manifestations of vessel dilation or occlusion become apparent, few data exist regarding the gene expression of cytokines or chemokines in relation to overexpression of MMPs.[7,8] Such evidence may contribute to our understanding of the role of cytokines and their receptors, protective or not protective, in the clinical course of vascular disease. In the present study, the gene expressions of cytokines and their receptors were systematically examined

(Received May 19, 2005; revised manuscript received August 26, 2005; accepted September 7, 2005)

*Divisions of Cardiovascular Medicine and Bioscience, *Biotechnology in Bioscience, **Pathology, †Cardiovascular Surgery, ††Neurosurgery and ‡Regenerative Medicine and Tissue Engineering, National Cardiovascular Center and Research Institute, Suita, Japan*

Part of this work was presented at the 53rd American College of Cardiology Annual Scientific Session in 2004, New Orleans, USA, and Plenary Session, 68th Annual Scientific Session of Japanese Circulation Society in 2004, Tokyo, Japan.

Mailing address: Masakazu Yamagishi, MD, PhD, FACC, Division of Cardiovascular Medicine and Bioscience, National Cardiovascular Center, 5-7-1 Fujishiro-dai, Suita 565-8565, Japan. E-mail: myamagi@hsp.ncvc.go.jp

using cDNA macroarray and then quantitatively evaluated with real-time reverse transcription polymerase chain reaction (RT-PCR) methods.

Methods

Patients and Tissue Sampling

The protocol of this study was approved by the institutional committee for ethical review. Written informed consent was given by all patients. Tissue samples were obtained from 31 patients who underwent elective graft replacement for AAA with a diameter of 58±18 mm by computed tomography (29 males, 2 females; mean age, 71±2 years) and from 24 patients who underwent carotid endarterectomy for severe stenosis (>90% diameter stenosis by angiography) of the extracranial carotid artery (all males; mean age, 68±2 years). As for medical treatment, 20 patients with AAA and 10 with CAS were treated with 3-hydroxy-3-methylglutaryl coenzyme A (HMG-CoA) reductase inhibitors, and 17 with AAA and 7 with CAS were with angiotensin-converting enzyme inhibitors or angiotensin II receptor blockade.

During graft replacement for AAA, a strip of aortic wall that contained the dilated region and relatively normal portion was carefully excised. Carotid endarterectomy was extended in a caudal direction to include a sample of minimally affected common carotid artery proximal to the plaque but in continuity with it, to act as a paired control. After removing part of the tissue for histological examination, all the samples were quickly frozen in liquid nitrogen and stored at –80°C until extraction of RNA.

RNA Preparation and cDNA Synthesis

Experimental procedures have been already described elsewhere[2]. Briefly, the samples were homogenized in 1.0 ml ISOGEN™ reagent (Nippon Gene, Tokyo, Japan), thoroughly mixed with 0.2 ml chloroform and centrifuged at 15,000 G for 15 min at 4°C. The aqueous supernatant was transferred into a micro test tube, mixed with 0.6 ml isopropanol and centrifuged at 15,000 G for 15 min at 4°C. The precipitated total RNA was rinsed with 70% ethanol, air-dried, and then resuspended in RNase-free water. The concentration of the extracted total RNA was assessed using spectrophotometry. Next, the total RNA was treated with DNase Free™ reagent (Ambion, Austin, TX, USA) for 60 min, and then reverse-transcribed with Superscript II™ (Invitrogen, Carlsbad, CA, USA) at 37°C for 60 min using Random Primer™ (TaKaRa, Tokyo, Japan). The resultant cDNA mixture was stored in small aliquots at –20°C until further use. The integrity of each cDNA mixture was checked by amplification of glutaraldehyde 3-phosphate dehydrogenase (GAPDH) with ExTaq™ (TaKaRa), using the primer set 5'-ACCACAGTCCATGCCATCAC-3'/5'-TCCACCACCCTGTTGCTGTA-3'.

Complementary DNA Macroarray

Labeled cDNA probes were prepared with reagents provided with the Atlas Human Array kit (Clontech Laboratories, Palo Alto, CA, USA). For each specimen, 2.5 μg of total RNA was incubated with Human Cytokine-Specific Primers (R&D Systems, Minneapolis, MN, USA) for 5 min at 65°C and then at 41°C. A mixture of reaction buffer, dNTP mix, 50 U of Moloney murine leukemia virus reverse transcriptase and [α-^{32}P] dATP (Amersham Pharmacia Biotech, Piscataway, NJ, USA) was added to each sample, which was then incubated at 41°C for 60 min. The labeled cDNA probes were purified with column chromatography to remove unincorporated isotope (ProbeQuant™ G-50 Micro Columns; Amersham Pharmacia Biotech).

A nylon membrane containing bound cDNA clones corresponding to 375 different human genes (Human Cytokine Expression Array; R&D Systems) was prehybridized with a solution of hybridization buffer (ExpressHyb; Clontech) and salmon testes DNA at 68°C. Each labeled cDNA probe was mixed into prehybridization buffer and incubated overnight at 68°C with a membrane. After hybridization, the membrane was washed with wash solution 1 (2×standard saline citrate (SSC), 0.1% sodium dodecyl sulfate (SDS)) and wash solution 2 (0.1×SSC, 0.1% SDS) at 68°C followed by a final wash of 2×SSC at room temperature. The washed membrane was wrapped in plastic wrap and exposed to a phosphor imaging screen. Imaging screens were scanned and analyzed with imaging software (Atlas Image software, Clontech). The signals on each array were corrected for background with an average for blank columns and standardized with a housekeeping gene present on the same membrane (glyceraldehyde phosphate dehydrogenase). The duplicated intensity signals for each gene were summed for data analysis. The ratio of gene expression levels was determined by dividing the signal intensity on the AAA array by that on the control array. Differential gene expression was considered significant when the signal ratio was greater than 5:1.

Primers and Probes for Real-Time RT-PCR

Using Primer Express software (Applied Biosystems, Foster, CA, USA), several sets of primers were designed for each of the genes. The primer set amplifying a target cDNA most effectively, which was evaluated by electrophoresis and staining with ethidium bromide, was selected for final use. Subsequently, the TaqMan probe inherent to each primer set was prepared, which was an oligonucleotide labeled with a reporter dye (FAM) at the 5'-end and a quencher dye (TAMRA) at the 3'-end.

Real-time RT-PCR was performed using an ABI PRISM™ 7700 Sequence Detection System (Applied Biosystems). The reaction solution was assembled in a volume of 25 μl, which comprised TaqMan™ Universal PCR Master Mix (Applied Biosystems), forward and reverse primers (final concentration 300 nmol/L each), TaqMan probe (final concentration 200 nmol/L) and cDNA mixture (≈2.5 ng). The conditions for real-time RT-PCR were preheating at 50°C for 2 min and at 95°C for 10 min, followed by 40 cycles of shuttle heating at 95°C for 15 s and at 60°C for 1 min. Throughout this study, the cDNA mixture from a particular sample was used to generate the working standard for quantitation of the cDNA of interest, which plots the relationship between the dilution of the standard cDNAs and the corresponding Ct value (the number of cycles necessary to obtain a threshold fluorescent signal). The initial quantity of the cDNA of interest in a certain cDNA mixture was calculated from the working standard and then normalized to that of GAPDH determined with TaqMan™ Assay Reagent Endogenous Control (Applied Biosystems). The normalized value for each target cDNA reflects the expression level of the corresponding gene in a test sample relative to the standard tissue.

Histology and Immunohistochemistry

Part of the plaque was placed in tissue fixative

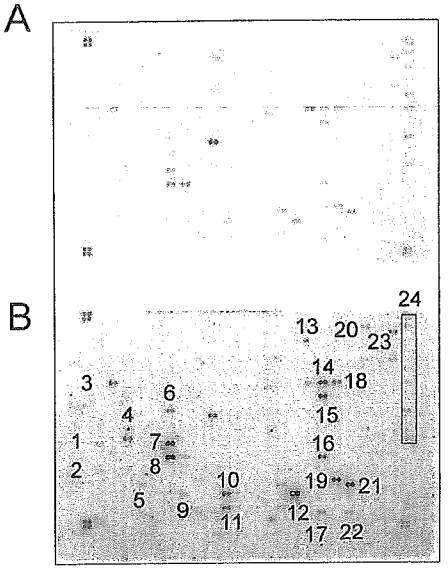

1:EpCAM
2:ICAM-3
3:Endothelin-2
4:SLAM
5:IL-8
6:CCR-5
7:CXCR-2
8:CXCR-5
9:Pleiotrophin
10:EphrinA3
11:EphrinA5
12:CNTFRa
13:GFRa2
14:SPC-4
15:UrokinaseR
16:MMP-3
17:MMP-14
18:TIMP-1
19:ActivinRIA
20:BMPRIA
21:ActivinRIB
22:BMPRIIA
23:TNFRII
24:Housekeeping genes

Fig 1. Representative result of the cDNA macroarray of the tissue from an abdominal aortic aneurysm. (A) Control, (B) diseased tissue.

Table 1 Sequence of Primer and Probe

IL8 sense	*TCTAGGACAAGAGCCAGGAAGAA*
IL8 antisense	*GGCCAGCTTGGAAGTCATGT*
IL8 TaqMan	*CACCGGAAGGAACCATCTCACTGTGTGTA*
CXCR2 sense	*TACATGGCTTGATCAGCAAGGA*
CXCR2 antisense	*GCCCTGAAGAAGAGCCAACA*
CXCR2 TaqMan	*TGCCCAAAGACAGCAGGCCTTCCT*
CCR2 sense	*GCCGCTGCTCATCATGGT*
CCR2 antisense	*TGCCTCTTCTTCTCGTTTCGA*
CCR2 TaqMan	*ACTCGGGAATCCTGAAAACCCTGCTTC*

The sequences of the primer and probe of MCP-1 were provided by on-line TaqMan gene expression assays (Assay ID Hs 00234140_m1).

(Histochoice, Hedwin, Baltimore, MD, USA). After overnight fixation, the samples were paraffin embedded and sectioned at 4 μm intervals. Tissue sections were deparaffinized with xylene followed by immersion in graded alcohol. They were washed 3 times for 5 min each in phosphate-buffered saline (PBS) and blocked with bovine serum albumin for 60 min. Specimens were then incubated with primary antibodies (Fuji Chemical, Tokyo, Japan) overnight at 4°C. After they were washed in PBS, specimens were incubated with biotinylated rabbit anti-mouse IgG for 60 min at room temperature. Specimens were then washed with PBS, stained with horseradish peroxidase-conjugated streptavidin, and finally incubated with substrate solution for 1–15 min. The tissue sections were also stained with hematoxylin-eosin.

Statistical Analysis

The mean and standard error of triplicate data are presented. Statistical analysis was performed by Mann-Whitney test and Wilcoxon signed-rank test using Stat View 5.0 software (Abacus Concepts, Calabasus, CA, USA) on a Macintosh computer. A p-value <0.05 was considered significant.

Results

cDNA Macroarray for AAA Tissues

A representative autoradiograph of the human cytokine expression array after hybridization with cDNA probes derived from AAA and adjacent control tissues is shown in Fig 1. Although densitometric analysis revealed significant (>5-fold) upregulation of 97 of the 375 genes, 23 genes appeared to be overexpressed by visual inspection. Under these conditions, 10 cytokine-related genes were strongly overexpressed in comparison with those in the adjacent control tissues: Activin R1A (TGF b superfamily, 13:1), Activin R1B (TGF b superfamily, 12:1), BMP RIIA (TGF b superfamily, 12:1), CXCR-5 (chemokine receptor, 12:1), CXCR-2 (chemokine receptor, 11:1), IL-8 (chemokine, 9:1), CCR-6 (chemokine receptor, 9:1), BMP RIA (TGF b superfamily, 8:1), CXCR-1 (chemokine receptor, 7:1), and CXCR-6 (chemokine receptor, 7:1). It was interesting that IL-8 and its receptor, CXCR-2, were simultaneously upregulatated, suggesting their significant role in disease development. Therefore, these 2 genes were quantitatively determined by real-time RT-PCR with TaqMan probes (Table 1). Additionally, in some patients the expressions of MCP-1 and its receptor, CCR-2, were determined by the same procedures.

In AAA, the expression of IL-8 and CXCR-2 in CAS was 0.53±0.16 and 2.04±0.75, respectively and significantly greater than those in the adjacent control tissues in which the expressions were 0.11±0.04 and 0.29±0.10 ($p<0.01$), respectively. Under these conditions, the expressions of MCP-1 and CCR-2 in the diseased portion were slightly upregulated at 1.51±0.38 and 1.24±0.10, respectively, in comparison with those in adjacent control tissues (0.32±0.08 and 0.28±0.09, respectively, n=4).

In CAS, expression of IL-8 and CXCR-2 in CAS was 1.35±0.25 and 2.00±0.51, respectively and significantly greater than that in the adjacent control tissues where it was 0.60±0.16 and 0.58±0.21 ($p<0.05$), respectively (Fig 2). Under these conditions, there was no statistical significance

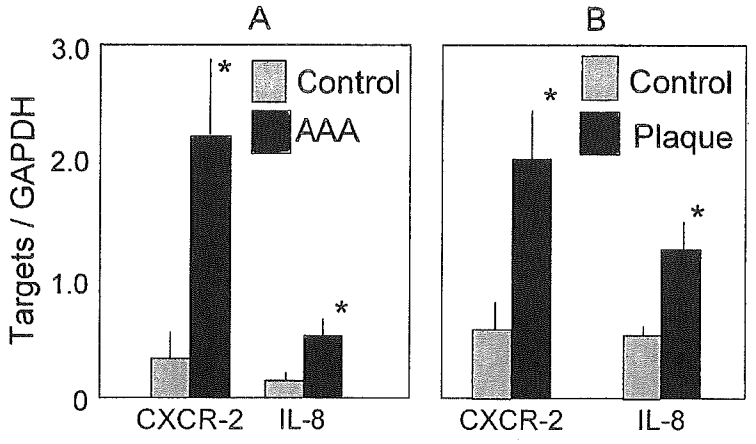

Fig 2. Expression of CXCR-2 and interleukin (IL)-8 in (A) abdominal aortic aneurysm (AAA) and (B) carotid artery stenosis (CAS).

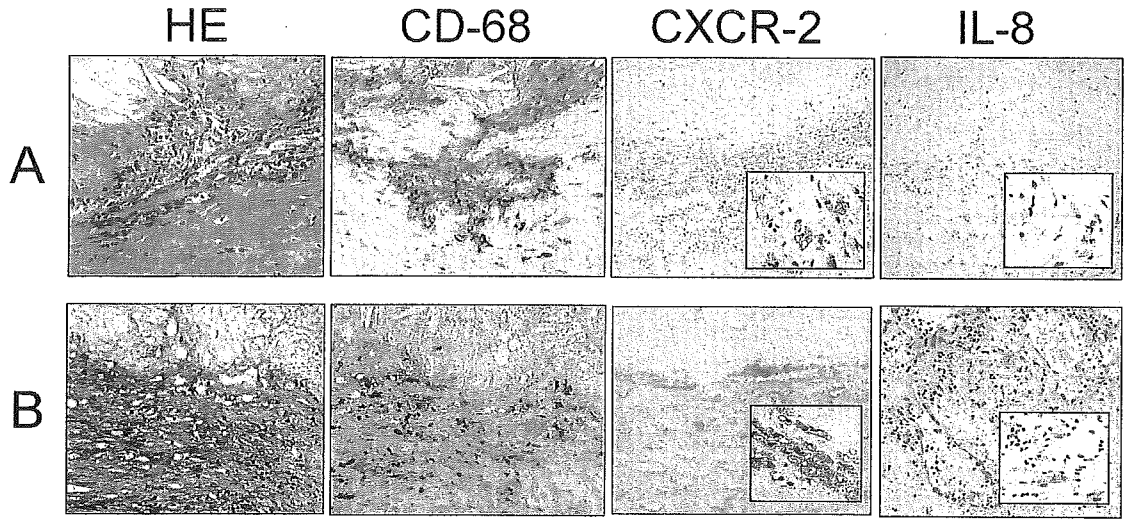

Fig 3. Immunohistochemisty of tissue samples from (A) abdominal aortic aneurysm and (B) carotid artery stenosis (Original magnification ×100; Insert: ×400).

in the expressions of MCP-1 and CCR-2 in diseased (0.44±0.15 and 2.72±1.76, respectively) and control (0.38± 0.11 and 0.99±0.18, n=13) tissues.

Immunohistochemistry

In both AAA and CAS tissues, the control regions exhibited mild atherosclerosis in which a few CD-68 positive macrophages existed. The specimens of AAA consisted of thinned or thickened vascular tissue in which typical atheromatous plaques with infiltration of macrophages and lymphocytes were present. Plaque regions of CAS mainly consisted of a lipid-rich core and fibrous tissue in which CD-68 positive macrophages had accumulated, particularly in the shoulder regions of the atheroma. Under these conditions, IL-8 and CXCR-2 were mainly expressed in the macrophages, which were identified as CD68-positive cells in each tissue (Fig 3).

Discussion

In the present study, we used cDNA macroarray to try and determine the possible cytokine-related mediators that could contribute to the development of atherosclerosis, and we then quantitatively measured the expression of their mRNA using real-time RT-PCR. The inflammatory chemokine IL-8 and its receptor, CXCR-2, were demonstrated to be simultaneously upregulated in the diseased portions, suggesting their key role in the development of dilated and occlusive atherosclerotic diseases.

Determination Procedures for mRNA

The recent development of microchip- or membrane-based cDNA arrays has enabled examination of the simultaneous expression of multiple gene products of known identity, facilitating the identification of altered patterns of gene expression in a given tissue[9] Because this approach has the potential to reveal novel pathophysiologic insights, we first used it to characterize the simultaneous expression of approximately 375 gene products in human AAA, in which enough mRNA was collected to synthesize the cDNA, and to compare the expression profile of AAA with adjacent control tissues. We found that the expression of IL-8 (9-fold) and its receptor, CXCR-2 (11-fold) were simultaneously upregulated in the diseased portion.

However, it is necessary to reemphasize that the cDNA array is most valuable for detecting novel, unanticipated